

Research Article

Study on Mesoscopic Mechanics of Recycled Asphalt Mixture in the Indirect Tensile Test

Yanping Sheng,¹ Haichuan Jia ,¹ Hongli Lv,² Huaxin Chen ,¹ Xiaorui Zhao,¹ Runzhi Wang,¹ and Jiandang Meng²

¹School of Material Science and Engineering, Chang'an University, Xi'an 710064, China

²Management Office of Puyang to Hebi Highway Section, Division of Highway, Henan Department of Transportation, Henan 410902, China

Correspondence should be addressed to Haichuan Jia; hcjia1117@163.com and Huaxin Chen; hxchen@chd.edu.cn

Received 24 October 2020; Revised 25 November 2020; Accepted 26 November 2020; Published 18 December 2020

Academic Editor: Fulu Wei

Copyright © 2020 Yanping Sheng et al. This is an open access article distributed under the Creative Commons Attribution License, which permits unrestricted use, distribution, and reproduction in any medium, provided the original work is properly cited.

Reclaimed asphalt pavement (RAP) mainly contains asphalt binder and aggregates, and the RAP materials used in paving roads could save virgin materials. This paper studied the following: asphalt mixture with different RAP material contents was prepared; then the indirect tensile test was carried out, and the mesoscopic model of the recycled asphalt mixture was reconstructed digitally. Discrete element method (DEM) of indirect tensile test was carried out to analyze the mechanical properties of recycled asphalt mixture in mesoscopic perspective. The results showed that there were some gaps between the simulation result of the digital specimen model and the test value of the recycled asphalt mixture, but the velocity vector and the law of force chain development of the recycled asphalt mixture could be explained in mesoscopic perspective. It proved that the virtual simulation test of the mechanical test was effective. The damage process of recycled asphalt mixture was analyzed in mesoscopic perspective, and the unification of mechanical response and macroscopic appearance was completed. Meanwhile, the simulation method of mesoscopic mechanics was an effective supplement to traditional tests, and guided tests method theoretically.

1. Introduction

Asphalt pavement is used widely in the construction of highways in the world because of its excellent performance [1]. However, the service life of asphalt pavement could be affected by severe climate and overload [2–4]. The environmental condition and repeated load lead to pavement distress such as fatigue cracking, permanent deformation, low-temperature cracking, and moisture damage. Then, the damaged asphalt pavements are discarded, resulting in a lot of waste of resources. The resource conservation and environmental problems attracted attention and became the focus in more research [5, 6]. Recycled asphalt and aggregate are used in asphalt pavement, saving the use of aggregate and asphalt in paving roads. RAP materials from damaged asphalt pavements contain asphalt and aggregate. Moreover, the use of RAP materials in asphalt pavement reduces the consumption of raw materials (asphalt and aggregate) and

saves resources. The fatigue and cracking properties of recycled asphalt mixtures decline compared with hot mix asphalt (HMA) because of aged bitumen and reduction in brittleness of the mixtures containing high RAP contents. Additionally, aging in asphalt and secondary aging of RAP materials may happen due to excessive construction temperature [7–12]. Hence, the RAP material contents used in recycled asphalt mixtures are generally less than 30%. Furthermore, the tensile strength, resistance to rutting, low-temperature cracking, and fatigue cracking of recycled asphalt mixture should be concerned.

Montanez [13] studied the rheological properties, mechanical properties, and moisture damage of fine aggregates from different RAP material sources and evaluated the differences between RAP materials. The results showed that the single source of RAP materials or the homogenization process between different RAP material sources was significant for manufacturing HMA. Goli [14] used indirect

tensile strength, indirect tensile fatigue failure, semicircular bending, and dynamic creep tests to study the effect of moisture damage on the performance of asphalt mixtures. The results showed that the warm mix asphalt containing RAP materials has hydrophilicity, moisture sensitivity, and aging properties but has an inhibitory effect on the influence of moisture performance. Rathore [15] evaluated the asphalt mixing parameters (mixing temperature, mixing time, and equipment) of recycled asphalt mixture with high RAP content using the indirect tensile strength and the stiffness modulus test. The results showed that mixing and heating temperature were important parameters in producing recycled asphalt mixture. Zhu [16] examined the performance of high modulus asphalt mixture containing RAP materials including high-temperature performance, low-temperature performance, and moisture susceptibility. The fatigue and crack behavior of recycled asphalt mixture are significant design indexes, which affects the use of pavement. In previous studies, the long-term life of recycled asphalt pavement was considered through indirect tensile strength test, fatigue failure test, semicircular bending test, and modulus tests. Scientists and engineers studied that the mechanical properties of recycled asphalt mixtures were affected by the use of regenerants, the content of RAP materials, and environmental conditions. Furthermore, the indirect tensile test obtains the failure strength and deformation parameters to evaluate the mechanical properties of the material. However, the composition structure of the recycled asphalt mixture is more complex and uneven compared with HMA [17]. Thus, the indirect tensile test is difficult to define the internal damage law of the asphalt mixture accurately.

Meanwhile, the mesoscopic mechanics method provides the way for the study of the mechanical behavior of asphalt mixtures. Numerical simulation is an effective method to research the occurrence and development of cracking in asphalt mixtures. At present, there are two different numerical methods used extensively for such investigations: finite element method (FEM) and discrete element method (DEM). The FEM represents discrete elements in the actual continuous domain and was widely used to study the cracking behavior of homogeneous materials using the continuum mechanics theory [18]. However, asphalt mixtures are discontinuous in material distribution and mechanical parameters. Therefore, the microcracking of asphalt mixture is difficult to simulate based on the FEM accurately. DEM uses explicit difference algorithms for mechanical research in mesoscopic perspective, which is suitable for studying the force of granular mixture. It decomposes the asphalt mixture into spherical elements or disks elements of unit thickness, which quantify the internal stress of the asphalt mixture during loading [19, 20]. Moreover, it reflects the particle properties and discontinuous characteristics of asphalt mixtures. Compared with continuum mechanics, DEM is a simulation method to research asphalt mixture with heterogeneous and particulate characteristics [21–23].

Wu [24] modified asphalt mixtures with styrene-butadiene-styrene (SBS) and established the DEM model of AC-16 asphalt mixture. During the grinding process,

asphalt mixture was avoided from being broken into large pieces considering reducing the damage of the aggregate. Ma [25] researched the air void of the asphalt mixture during the compaction process and the characteristics of the mesoscopic structure changes. DEM was used to establish a numerical simulation method for compaction considering critical particle size and boundary effects in the study. Wang [26] researched that the simplified viscoelastic continuum damage model was used to characterize the recycled asphalt pavement according to the material properties, traffic load, and climatic conditions, and the result showed that the theoretical performance predictions matched the field performance. Qian [27] investigated the Marshall impact compaction and static compaction methods by using DEM simulation to evaluate the compacting effects of the compaction process. In the compaction process, the size distribution of particles was unevenly distributed in a horizontal direction due to the large size particles (>16 mm) being difficult to move in the dense specimen. Yu [28] studied that the DEM was used to investigate the effect of aggregate size and angularity distribution on dynamic modulus, which evaluates the aggregate effect on fatigue and rutting performance and provides the guide to improve the mixing design. Researches showed that DEM is used to simulate the compaction of the specimen and then simulate the performance test. The method is scientific and could complete experimental conditions that cannot be achieved in the laboratory.

As the heterogeneous and particulate mixture, recycled asphalt mixture is the discontinuous medium material with complex components. Many scholars researched the traditional properties of recycled asphalt mixtures, but there is little research on the analysis of the mesoscopic damage evolution of recycled asphalt mixtures based on the DEM. In this study, the indirect tensile tests of recycled asphalt mixture with different RAP material contents were conducted, then the mesoscopic model of the recycled asphalt mixture was reconstructed digitally based on DEM, and the simulation method was used to research the mesoscopic damage of recycled asphalt mixture. The objective of this paper is to research the damage process of recycled asphalt mixture in mesoscopic perspective and carry out the unification of mechanical behavior and macroscopic appearance to supplement the traditional tests effectively. The flow chart of research is presented in Figure 1.

2. Materials

2.1. Asphalt Binder and Aggregate. SK-90# asphalt was used in the test, and its properties are shown in Table 1. The penetration (25°C), specific gravity (15°C), ductility (15°C), softening point, and residual penetration ratio (25°C) test were conducted according to the Standard Test Methods of Bituminous Mixtures for Highway Engineering of China (JTG E20-2011) [29]. Additionally, the aggregate with the nominal maximum aggregate size (NMAS) of 16 mm was selected, and the indexes are shown in Table 2.

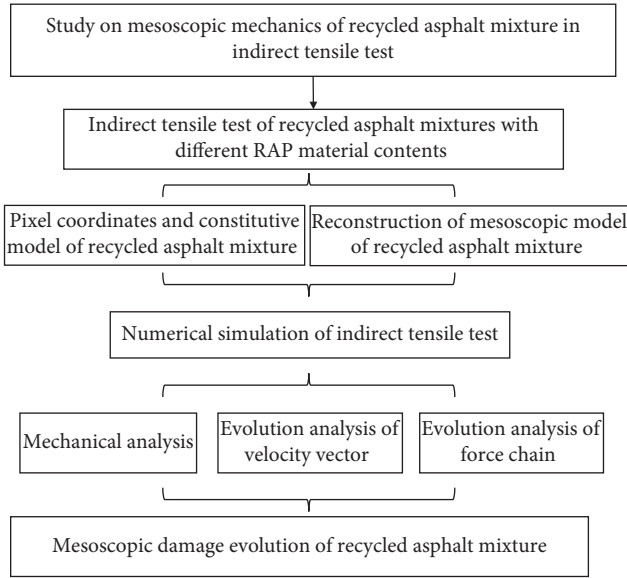


FIGURE 1: The research plan chart.

TABLE 1: Technical properties of SK-90# asphalt binder.

Test	Unit	Result	Standard
Penetration test (25°C, 5s, 100g)	0.1 mm	95	T0604
Ductility test (15°C)	cm	>100	T0605
Softening point (°C)	°C	44.5	T0606
Solubility	%	99.62	T0607
Specific gravity (15°C)	g/cm ³	1.030	T0603
Mass loss	%	0.4	T0609
RTFOT Residual penetration ratio (25°C)	%	57.8	T0604
Ductility (10°C)	cm	12	T0605

TABLE 2: Technical properties of Aggregate.

Test	Unit	Result	Standard
Coarse aggregate specific gravity	g/cm ³	2.758	T0304
Fine aggregate specific gravity	g/cm ³	2.746	T0328
Water absorption	%	1.02	T0304
Crush value	%	19.8	T0316
Los Angeles abrasion value	%	19.1	T0317
Flakiness	%	2.6	T0312
Sand equivalent	%	1	T0310

2.2. *RAP Materials and Rejuvenator.* The RAP materials of Gonghe-Yushu Expressway in Qinghai Province were separated by centrifugal separation, and the asphalt content was 5.13%. Meanwhile, the trichloroethylene solvent extraction method was used to collect the aggregates. The sieving results of RAP materials are shown in Table 3. The RAP material contents of 0%, 15%, 30%, 45%, and 60% in recycled asphalt mixture corresponded to the optimum asphalt content of 4.72%, 4.87%, 4.81%, and 4.71%, respectively. And the optimum rejuvenator content was 0.2% of RAP material contents. The Marshall design method was used for grading design, and the aggregate grading is shown in Figure 2.

3. Numerical Simulation in Discrete Element Method

The two-dimensional particle flow code (PFC2D) is mainly based on numerical methods, using circular particle elements to simulate the motion and interaction of the particle medium to perform numerical simulation analysis, then the simulation results of local elements are used to research the constitutive model of overall material calculation [30]. Furthermore, the explicit difference algorithm and the mesoscopic mechanics in the discrete element theory were used to analyze the overall mechanical properties of the materials. In this paper, the digital model for the indirect tensile test of recycled asphalt mixtures was established, and the servo mechanism was used to control the load application of the digital specimen, then the mesoscopic damage changes of the specimen were tracked during the loading process. The difference between the numerical simulation and the experimental results was compared, and the feasibility of the DEM was verified [31–34]. A binary image of the cross section of specimen was obtained as the numerical simulation object of the indirect tensile test and is shown in Figure 3. The pixel coordinates of the aggregates, reclaimed aggregates, and asphalt mortar were extracted, and the coordinate reading of the mesoscopic model was completed. Then, the coordinates of each component were imported into the discrete element software to generate a two-dimensional digital sample of the recycled asphalt mixture. The coordinated results of aggregates, reclaimed aggregates, and asphalt mortar are shown in Figure 4.

3.1. *Constitutive Model.* In Figure 5, the constitutive models in PFC2D include stiffness model, sliding model, and bonding model. Moreover, the stiffness model is the relationship between contact force and relative displacement, the sliding model is the relationship between tangential and normal contact forces (two contacting particles may relatively slide), and the bonding model imposes constraints on the contacting particles. What is more, the mesoscopic model included an internal contact of aggregate, aggregate-aggregate contact, reclaimed asphalt mortar-aggregate contact, and internal contact of reclaimed asphalt mortar. Burger’s model is used to describe the viscous behavior of the asphalt mixtures, which is the combination of Kelvin model (spring and dashpot in parallel) and Maxwell model (spring and dashpot in series). The Kelvin model describes creep and creep recovery behavior, and the Maxwell model describes the mechanical behavior of stress relaxation. After the two models are connected in series, the creep and stress relaxation characteristics of the material could be described, which is suitable for the force analysis of viscoelastic materials. Additionally, the aggregates and reclaimed aggregates are regarded as elastic materials, and their constitutive mechanical properties are characterized by the spring model [35, 36]. The contact inside the aggregate and between adjacent aggregates is described by a linear contact model, which is characterized by two springs connected in series, as

TABLE 3: Gradation of RAP materials.

Size (mm)	16	13.2	9.5	4.75	2.36	1.18	0.6	0.3	0.15	0.075
Passing (%)	100.00	94.43	77.20	43.82	28.54	21.19	15.70	11.54	7.91	4.61

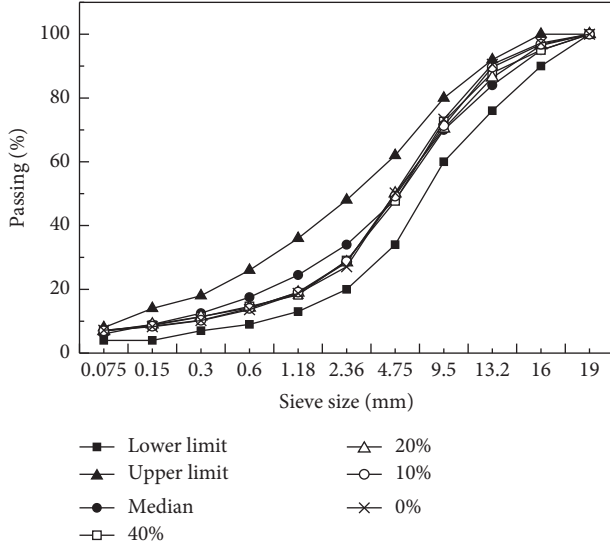


FIGURE 2: The aggregate grading of asphalt mixture.



FIGURE 3: Binary image.

shown in Figure 5(c). What is more, the stiffness model at the contact point of the reclaimed asphalt mortar is described by the Burgers model in the normal and shear directions, as shown in Figure 5(a). The stiffness model of the contact between the aggregate and the reclaimed asphalt mortar is made up of the spring element and the Burgers model in series, as shown in Figure 5(b). Meanwhile, the aggregates and reclaimed aggregates were represented by spring element, and the reclaimed asphalt mortar was represented by the Burgers model. The sliding model at all contact points is expressed by the friction coefficient μ , and the bonding model is expressed by the tensile strength and the shear strength.

3.2. Model Reconstruction in DEM Simulation. In the mesoscopic model, the irregular aggregates and reclaimed asphalt mortar are composed of disks with single particle size. For example, in the cross section of the recycled asphalt mixture with 40% RAP materials, the cross section of the digital sample was composed of 11277 disks discrete element particles. The number of basic units constituting the aggregate was 5026, the number of basic units of the reclaimed aggregate was 1989, and the number of basic units of the reclaimed asphalt mortar was 4262. The generated two-dimensional digital specimen of the recycled asphalt mixture is shown in Figure 6.

With the mesoscopic structure of the recycled asphalt mixture, the mesoscopic parameters of the two-dimensional digital specimen model of the recycled asphalt mixture were set up, as shown in Tables 4 and 5. According to the two-dimensional digital model, the bond strength of the digital specimens was 4%. The bonding stiffness of digital specimens with 0%, 10%, 20%, and 40% RAP material was selected as 4, 1, 0.5, and 1, respectively. And the friction coefficients μ were 0.5, 0.3, 0.1, and 0.1, respectively. The indirect tensile test of asphalt mixture is to apply load to the cylindrical specimen of a specified size at the loading speed. And a dial indicator is used to measure the vertical and horizontal deformation of the specimen until the specimen is split and destroyed. The indirect tensile test of the two-dimensional digital specimen of recycled asphalt mixture was carried out by controlling the loading plate to load at 1 mm/min rate. The FISH language functions were used for secondary program development, and the servo mechanism control load application was carried out, tracking and monitoring the development of stress-strain, velocity vector, and force chain. The sample model after setting the loading plate is shown in Figure 7.

The constitutive relationship of Burger's contact model is expressed by

$$\begin{aligned}
 f_n &= C_{mn} \dot{u}_{mn} = u_k K_{kn} + \dot{u}_k C_{kn} = K_{mn} u_{mk}, \\
 f_s &= C_{ms} \dot{\delta}_{mc} = \delta_k K_{ks} + \dot{\delta}_k C_{ks} = K_{ms} \delta_{mk}, \\
 u_n &= u_k + u_{mk} + u_{mc}, \\
 u_s &= \delta_k + \delta_{mk} + \delta_{mc},
 \end{aligned} \tag{1}$$

where C_{mn} , C_{ms} , C_{kn} , C_{ks} —dashpot viscosity; K_{kn} , K_{ks} , K_{mn} , K_{ms} —spring stiffness; u_{mk} , δ_{mk} —the spring displacement of Maxwell model element in normal and shear direction; u_{mc} , δ_{mc} —the dashpot displacement of Maxwell model element in normal and shear direction; f_n , f_s —normal and shear force at the contact point; u_n , u_s —normal and shear displacement at the contact point; u_k , δ_k —the displacement of Kelvin model element in normal and shear direction.

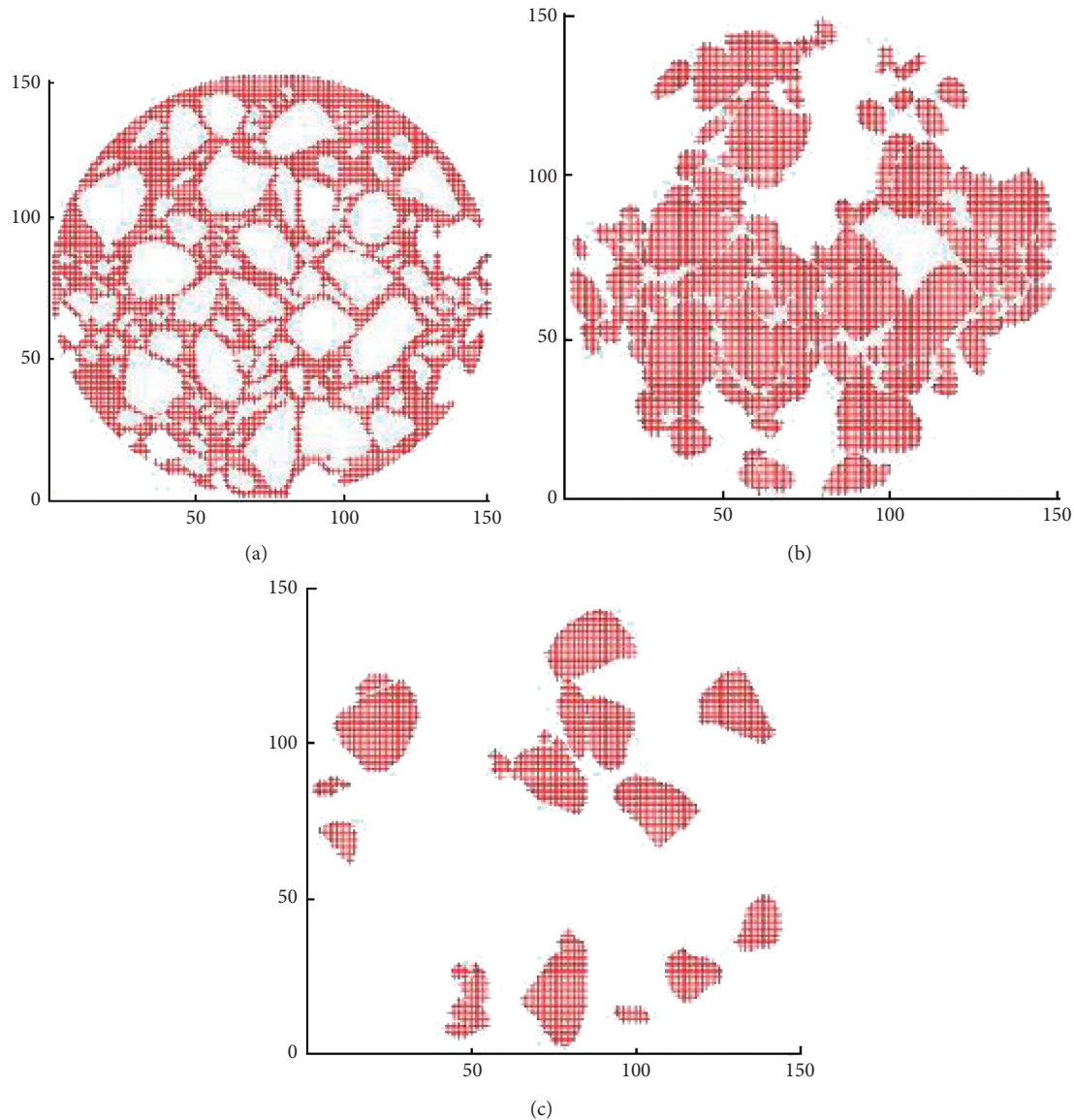


FIGURE 4: The coordinates of each component. (a) Asphalt mortar. (b) Aggregate. (c) Recycled aggregate.

4. Results and Discussion

4.1. Verification of the Discrete Element Model. As illustrated in Figure 8, there are differences between the discrete element simulation test and the test results. Because the parameters in the two-dimensional mechanical model were greatly simplified, resulting in a low consistency between the virtual model and test sample. What is more, in the mesoscopic model constructed by the DEM, the air void in the model was different from the test specimen. The components of the recycled asphalt mixture were complex, and the mesoscopic composition of structure was not clear, and the recognition of particle edge, binarization, and the coordinate reading of each component resulted in the loss of particle image information in the image processing. However, the overall simulation reflected the splitting strength value of the numerical specimens of recycled asphalt

mixture, which showed that the discrete element simulation of splitting strength test was feasible under certain conditions.

4.2. Velocity Vector Evolution Analysis. The indirect tensile test of the two-dimensional digital specimen was carried out by controlling the moving speed of the loading plate. The internal damage of the digital specimens with different RAP materials at the initial and completion loading was measured, respectively, which performed the failure process under the virtual test.

In Figure 9, the deformation of the digital specimen at the initial loading is mainly void compression. The voids were compressed during the initial loading, and the specimens reached the dense state. It showed that the mesoscopic performance of the digital specimens was consistent with the

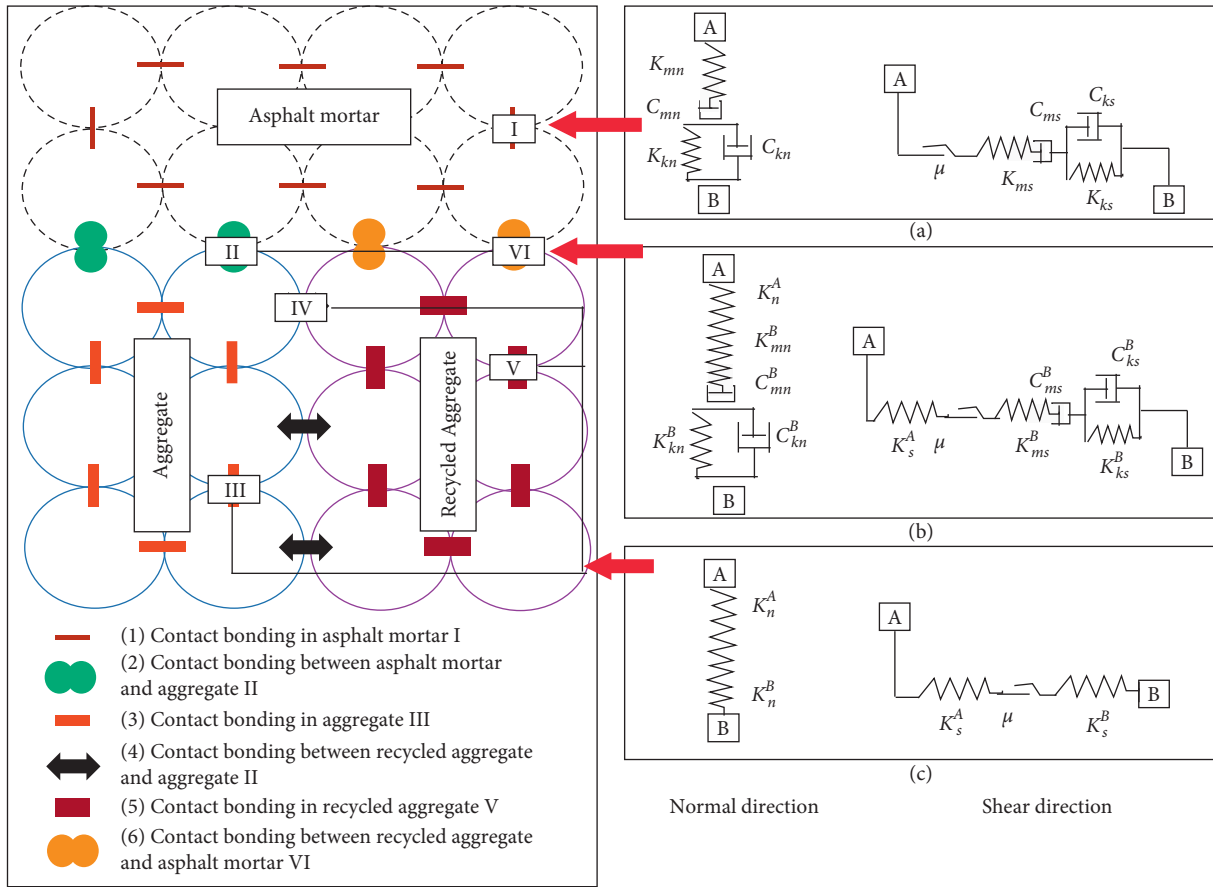


FIGURE 5: Constitutive model of recycled asphalt mixture.

macroscopic phenomenon. Furthermore, the compactness of digital specimens with different RAP material contents is different after initial loading. When the initial loading of specimen was completed, the color of the velocity vector area with the HMA was obviously lighter than that of others. On the other hand, the color of the specimen with 40% RAP materials was the darkest, and the sample had been deformed. During the simulation loading process, the HMA reached the dense state at the latest, but the compaction of digital specimen mixed with different RAP material contents was relatively faster. It showed that the digital specimen with higher RAP material contents could reach the compact state easily in the simulation test. At the same loading time step, when the compaction of specimen was faster, the pressure-bearing time would be longer, and the occurrence of cracks would be easier. Therefore, the addition of RAP materials to the asphalt mixture had an impact on the compactness. What is more, the crack resistance of the mixture decreased as the content of RAP materials increased.

Figure 10 shows that the specimens with different RAP material contents all have shear failure, and the shear surface has been marked in red in the figure. The digital specimens suffered shear failure when the load plate pressure reached the peak. Moreover, the shear failure surface was roughly divided into four directions and far away from the moving loading plate. And the failure surface was also shown as shear failure along a certain angle. The sample test and the

mesoscopic characterization of numerical model were almost coincident, which verified the reliability of the DEM. When the loading was completed, parts of the particles were scattered of the digital specimens with 0%, 10%, and 20% RAP materials, while more particles in the specimens with 40% RAP materials were scattered in the model area, and the damage was obvious. Because the specimen with 40% RAP materials had already been damaged before the stop node was controlled by the loading plate, the loading plate still applied load after failure, which caused the particles to rearrange and bear pressure randomly.

4.3. Evolutionary Law of the Force Chain. Figure 11 shows the contact force chain gradually running through the entire specimen as the load time increased. Below the loading plate, its force chain was mainly manifested as a pressure force chain, which extended in the vertical direction. In addition, the force chain on the outer edge of the specimen was mainly manifested as a tensile force chain distributed along the edge of the test specimen. At the same time, the particles contacted and transferred the load, and the internal pressure of the specimen was kept in a synchronized state. The edge area of tensile stress of the digital specimen with 40% RAP materials was obviously more than that of others in the initial loading, and the internal compressive stress area of the specimen had the wider influence range. It indicated that the

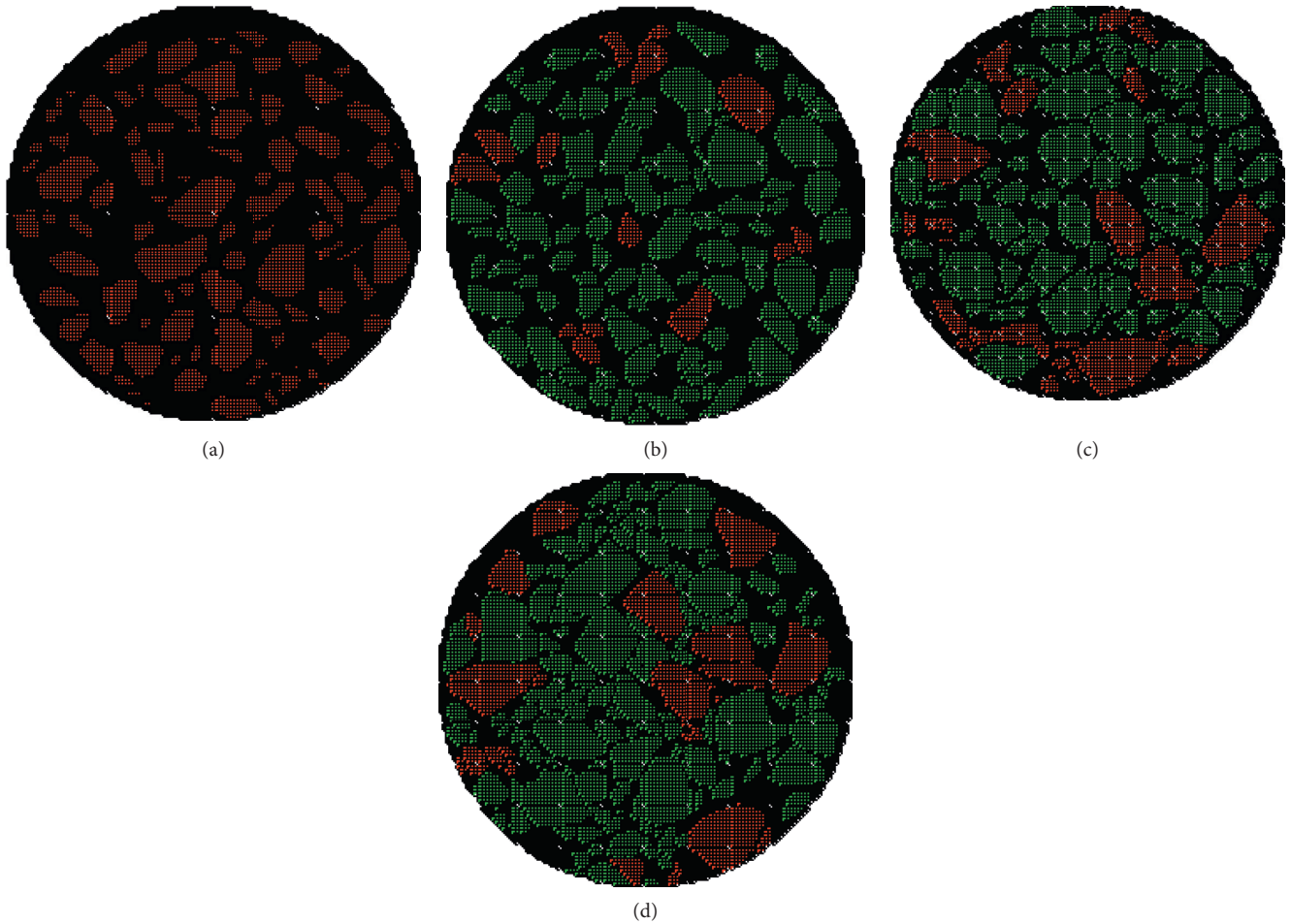


FIGURE 6: The two-dimensional digital specimen of the recycled asphalt mixture. (a) 0% RAP. (b) 10% RAP. (c) 20% RAP. (d) 40% RAP.

TABLE 4: Aggregate particle parameters.

Parameters	Density	Normal stiffness (particle)	Shear stiffness (particle)	Normal stiffness (contact)	Shear stiffness (contact)
Unit	kg/m ³	10 ⁹ N/m	10 ⁹ N/m	10 ⁹ N/m	10 ⁹ N/m
Value	2650	2.0	2.0	1.0	1.0

TABLE 5: Parameter values of Burger’s model.

Parameters	Value	
Maxwell	Normal stiffness (10 ⁹ N/m)	70.0
	Normal viscosity (Pa-s)	6.0
	Shear stiffness (10 ⁹ N/m)	25.0
Kelvin	Shear viscosity (Pa-s)	2.0
	Normal stiffness (10 ⁹ N/m)	4.0
	Normal viscosity (Pa-s)	0.5
	Shear stiffness (10 ⁹ N/m)	1.5
Shear viscosity (Pa-s)		0.1
Coefficient of friction		0.5

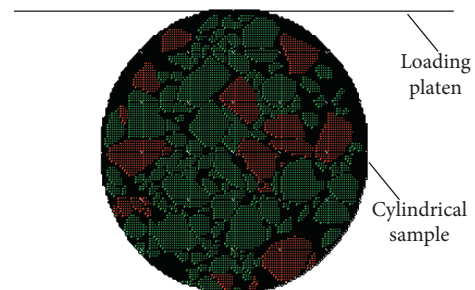


FIGURE 7: Loading model with specimen.

crack resistance of the digital specimen with 40% RAP materials was poor. The edge force chain of the HMA was tensile force, and the internal pressure force chain was mainly distributed. It was obviously better than the digital

specimen mixed with RAP materials, indicating that the crack resistance of the HMA was better than that of the recycled asphalt mixture. Therefore, the force chain distribution diagram showed the mechanical response of the

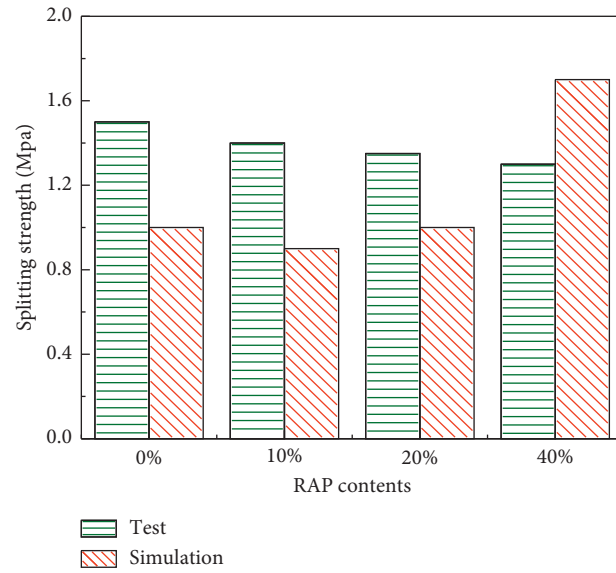


FIGURE 8: The discrete element simulation and experimental results.

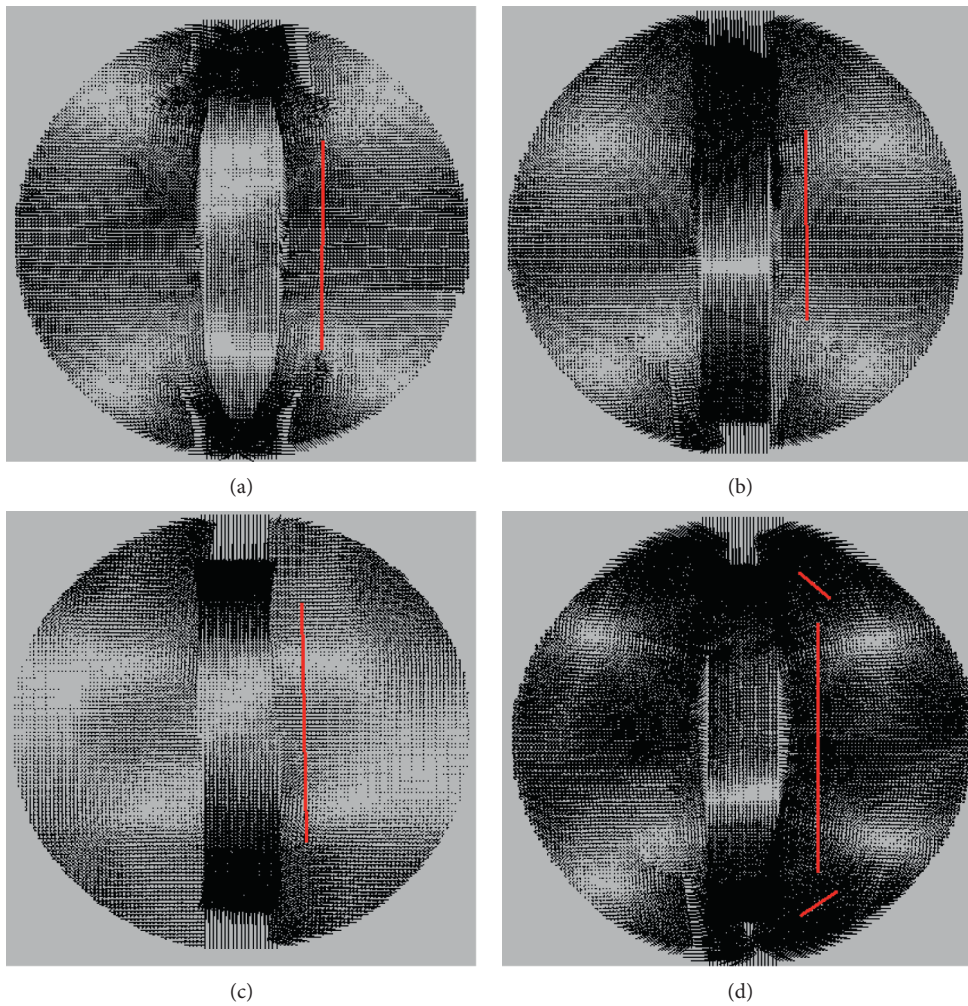


FIGURE 9: The vector diagram of specimens with different RAP content at the initial loading speed. (a) 0% RAP. (b) 10% RAP. (c) 20% RAP. (d) 40% RAP.

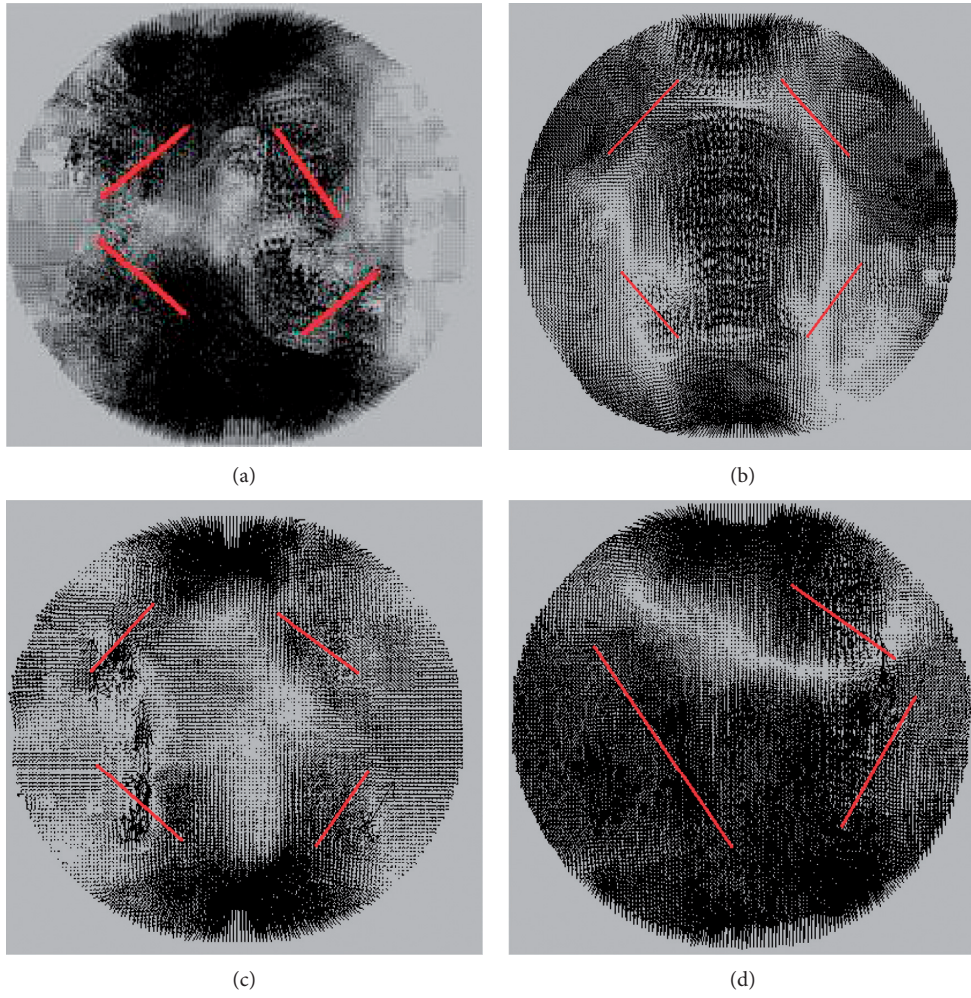


FIGURE 10: The vector diagram of specimens with different RAP material contents at the completed loading speed. (a) 0% RAP. (b) 10% RAP. (c) 20% RAP. (d) 40% RAP.

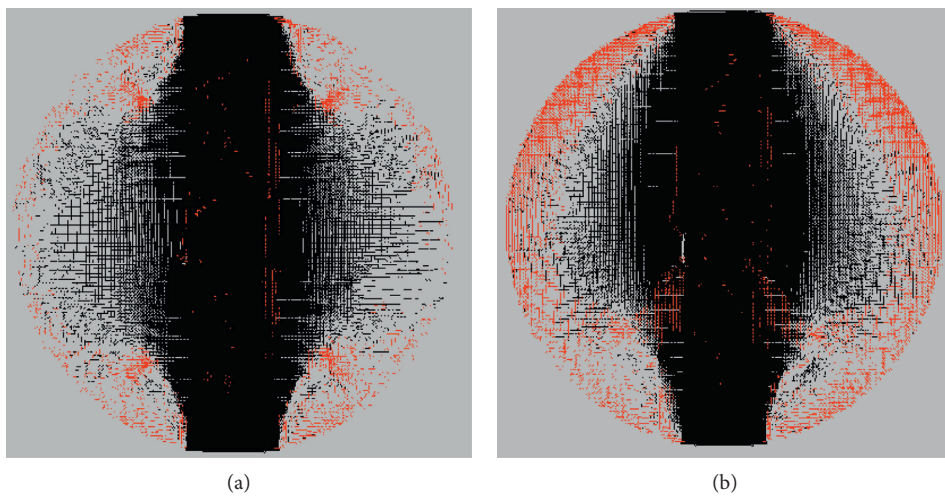


FIGURE 11: Continued.

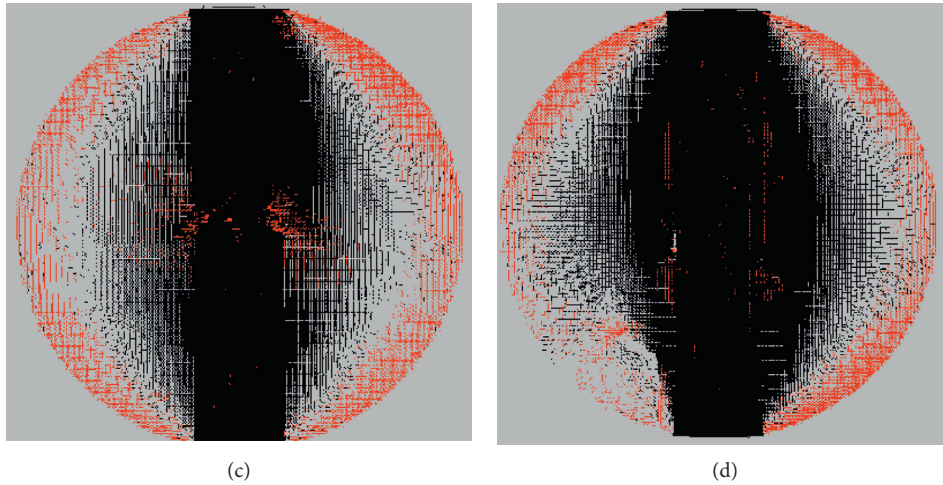


FIGURE 11: The force chain distribution diagram of specimens with different RAP material contents at the initial loading speed. (a) 0% RAP. (b) 10% RAP. (c) 20% RAP. (d) 40% RAP.

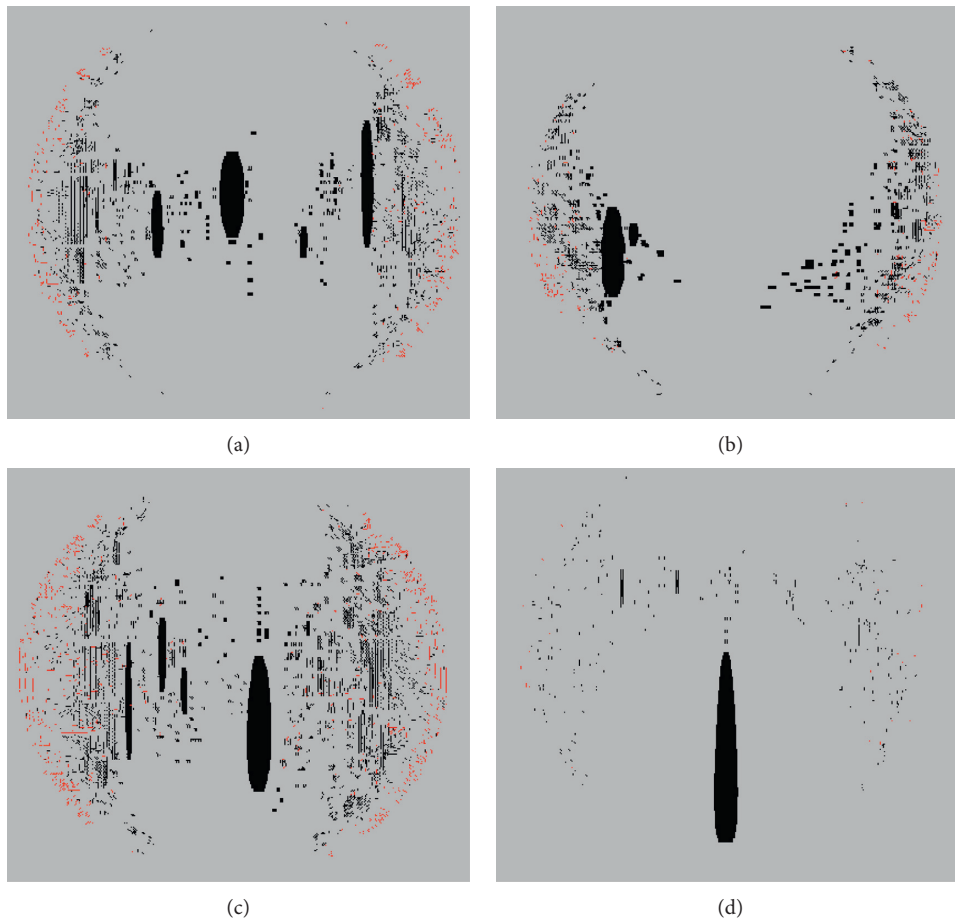


FIGURE 12: The force chain distribution diagram of specimens with different RAP material contents at the completed loading speed. (a) 0% RAP (b) 10% RAP. (c) 20% RAP. (d) 40% RAP.

indirect tensile test in mesoscopic perspective. Meanwhile, it explained the mesoscopic evolution rule of the indirect tensile test and was consistent with the macroscopic results.

As shown in Figure 12, when the test specimen is loaded completed, the digital test specimen all occurs shear failure. The contact force between the particles in

each test specimen gradually weakened, the particles separated under the loading, and the particles were rearranged randomly under the external loading. It could be shown that the internal particle contact force of the specimen with 40% RAP materials was more damaged than other specimens when the loading was completed. Furthermore, the disk units of the model were scattered around, parts of the aggregate particles were obviously broken, and the contact force chain disappeared. The macroscopic appearance of the indirect tensile test was that the specimen partially cracked at the initial loading. As the load increased, the cracks rapidly expanded to penetration, and the specimen eventually failed.

5. Conclusion

The indirect tensile simulation test explained internal damage law from mesoscopic perspective. It verified the feasibility of the DEM and provided the mesoscopic study of the traditional test method. The main conclusions are as follows:

- (i) The two-dimensional digital image reconstruction in DEM was carried out, and the model parameter was selected to complete the virtual mechanical test simulation of the digital reconstruction specimen.
- (ii) The indirect tensile simulation test results showed that there is still a certain gap with the laboratory test after the comparison of mesoscopic parameters. However, the simulation results could reflect the split strength of the numerical specimens.
- (iii) When the loading was completed, the specimen with 40% RAP materials was damaged more than other specimens. Meanwhile, more particles in the specimens with 40% RAP materials were scattered. The high RAP material contents in recycled materials will have a negative impact on the crack resistance of the mixture.
- (iv) The indirect tensile simulation test of recycled asphalt mixture explained the internal damage law in the mesoscopic perspective and provided a mesoscopic method of the traditional laboratory test method of recycled asphalt mixture.

Data Availability

The data used to support the findings of this study are included within the article.

Conflicts of Interest

The authors declare that they have no conflicts of interest.

Acknowledgments

This project was supported by the Science and Technology Project of Henan Department of Transportation (2020J-2-3).

References

- [1] L.-s. Gao, H.-c. Dan, and L. Li, "Response analysis of asphalt pavement under dynamic loadings: loading equivalence," *Mathematical Problems in Engineering*, vol. 2017, Article ID 7020298, 15 pages, 2019.
- [2] S. Sun, P. Li, J. Akhtar, J. Su, and C. Dong, "Analysis of deformation behavior and microscopic characteristics of asphalt mixture based on interface contact-slip test," *Construction and Building Materials*, vol. 257, 2020.
- [3] S. Lv, L. Hu, C. Xia et al., "Development of fatigue damage model of asphalt mixtures based on small-scale accelerated pavement test," *Construction and Building Materials*, vol. 260, 2020.
- [4] X. Ji, Y. Jiang, H. Zou, F. Cao, and Y. Hou, "Application of numerical simulation method to improve shear strength and rutting resistance of asphalt mixture," *International Journal of Pavement Engineering*, vol. 21, no. 1, pp. 112–121, 2018.
- [5] F. Yang, H. Li, G. Zhao, P. Guo, and W. Li, "Mechanical performance and durability evaluation of sandstone concrete," *Advances in Materials Science and Engineering*, vol. 2020, Article ID 2417496, 10 pages, 2020.
- [6] H. Li, W. Wang, W. Li, A. Taoum, G. Zhao, and P. Guo, "Replacement of limestone with volcanic stone in asphalt mastic used for road pavement," *Arabian Journal for Science and Engineering*, vol. 44, no. 10, pp. 8629–8644, 2019.
- [7] X. Zhu, Y. Sun, C. Du, W. Wang, J. Liu, and J. Chen, "Rutting and fatigue performance evaluation of warm mix asphalt mastic containing high percentage of artificial RAP binder," *Construction and Building Materials*, vol. 240, 2020.
- [8] Z. Xie, H. Rizvi, C. Purdy, A. Ali, and Y. Mehta, "Effect of rejuvenator types and mixing procedures on volumetric properties of asphalt mixtures with 50% RAP," *Construction and Building Materials*, vol. 218, pp. 457–464, 2019.
- [9] S. Mo, Y. Wang, F. Xiong, C. Ai, D. Wang, and G. Y. A. Tan, "Changes of asphalt fumes in hot-mix asphalt pavement recycling," *Journal of Cleaner Production*, vol. 258, 2020.
- [10] L. Gaillard, J. C. Quezada, C. Chazallon, and P. Hornych, "Resilient modulus prediction of RAP using the contact dynamics method," *Transportation Geotechnics*, vol. 24, 2020.
- [11] Y. Yan, R. Roque, C. Cocconcelli, M. Bekoe, and G. Lopp, "Evaluation of cracking performance for polymer-modified asphalt mixtures with high RAP content," *Road Materials and Pavement Design*, vol. 18, no. sup1, pp. 450–470, 2017.
- [12] Y. Yan, R. Roque, D. Hernando, and S. Chun, "Cracking performance characterisation of asphalt mixtures containing reclaimed asphalt pavement with hybrid binder," *Road Materials and Pavement Design*, vol. 20, no. 2, pp. 347–366, 2019.
- [13] J. Montañez, S. Caro, D. Carrizosa, A. Calvo, and X. Sánchez, "Variability of the mechanical properties of Reclaimed Asphalt Pavement (RAP) obtained from different sources," *Construction and Building Materials*, vol. 230, 2020.
- [14] H. Goli and M. Latifi, "Evaluation of the effect of moisture on behavior of warm mix asphalt (WMA) mixtures containing recycled asphalt pavement (RAP)," *Construction and Building Materials*, vol. 247, 2020.
- [15] M. Rathore and M. Zaumanis, "Impact of laboratory mixing procedure on the properties of reclaimed asphalt pavement mixtures," *Construction and Building Materials*, vol. 264, 2020.
- [16] J. Zhu, T. Ma, J. Fan, Z. Fang, T. Chen, and Y. Zhou, "Experimental study of high modulus asphalt mixture containing reclaimed asphalt pavement," *Journal of Cleaner Production*, vol. 263, 2020.

- [17] H. Ziari, A. Moniri, P. Bahri, and Y. Saghafi, "The effect of rejuvenators on the aging resistance of recycled asphalt mixtures," *Construction and Building Materials*, vol. 224, pp. 89–98, 2019.
- [18] D. Zhang, S. Hou, J. Bian, and L. He, "Investigation of the micro-cracking behavior of asphalt mixtures in the indirect tensile test," *Engineering Fracture Mechanics*, vol. 163, pp. 416–425, 2016.
- [19] F. Gong, Y. Liu, X. Zhou, and Z. You, "Lab assessment and discrete element modeling of asphalt mixture during compaction with elongated and flat coarse aggregates," *Construction and Building Materials*, vol. 182, pp. 573–579, 2018.
- [20] H. Feng, M. Pettinari, B. Hofko, and H. Stang, "Study of the internal mechanical response of an asphalt mixture by 3-D discrete element modeling," *Construction and Building Materials*, vol. 77, pp. 187–196, 2015.
- [21] F. Masi, I. Stefanou, V. Maffi-Berthier, and P. Vannucci, "A Discrete Element Method based-approach for arched masonry structures under blast loads," *Engineering Structures*, vol. 216, 2020.
- [22] Y. Wang, D. Zhang, L. Yang, T. Cui, H. Jing, and X. Zhong, "Modeling the interaction of soil and a vibrating subsoiler using the discrete element method," *Computers and Electronics in Agriculture*, vol. 174, 2020.
- [23] B. Owen, A. M. A. Nasar, A. R. G. Harwood, S. Hewitt, N. Bojdo, and B. Keavney, "Vector-based discrete element method for solid elastic materials," *Computer Physics Communications*, vol. 254, 2020.
- [24] J. Wu, D. Li, B. Zhu, and C. Wu, "Milling process simulation of old asphalt mixture by discrete element," *Construction and Building Materials*, vol. 186, pp. 996–1004, 2018.
- [25] T. Ma, Y. Zhang, D. Zhang, J. Yan, and Q. Ye, "Influences by air voids on fatigue life of asphalt mixture based on discrete element method," *Construction and Building Materials*, vol. 126, pp. 785–799, 2016.
- [26] Y. D. Wang, B. Keshavarzi, and Y. R. Kim, "Fatigue performance analysis of pavements with RAP using viscoelastic continuum damage theory," *KSCE Journal of Civil Engineering*, vol. 22, no. 6, pp. 2118–2125, 2018.
- [27] K. H. G. Qian, J. Li, X. Bai, and N. Li, "Compaction process tracking for asphalt mixture using discrete element method," *Construction and Building Materials*, vol. 235, 2020.
- [28] H. Yu and S. Shen, "Impact of aggregate packing on dynamic modulus of hot mix asphalt mixtures using three-dimensional discrete element method," *Construction and Building Materials*, vol. 26, no. 1, pp. 302–309, 2012.
- [29] JTG E20-2011, *Standard Test Methods of Bituminous Mixtures for Highway Engineering of China*, Ministry of Transport, Beijing, China, 2011.
- [30] Z. Zhang, W. Gao, K. Li, and B. Li, "Numerical simulation of rock mass blasting using particle flow code and particle expansion loading algorithm," *Simulation Modelling Practice and Theory*, vol. 104, 2020.
- [31] M. Baqersad, A. Hamed, M. Mohammadafzali, and H. Ali, "Asphalt mixture segregation detection: digital image processing approach," *Advances in Materials Science and Engineering*, vol. 2017, pp. 1–6, 2017.
- [32] S. Chen, Z. You, S.-L. Yang, A. Garcia, and L. Rose, "Influence of air void structures on the coefficient of permeability of asphalt mixtures," *Powder Technology*, vol. 377, pp. 1–9, 2021.
- [33] C. Nie, J. Li, and S. Wang, "Modeling the effect of spending on cyber security by using surplus process," *Mathematical Problems in Engineering*, vol. 2020, pp. 1–10, 2020.
- [34] P. K. Das, N. Kringos, and B. Birgisson, "Numerical study on the effect of mixture morphology on long-term asphalt mixture ageing," *International Journal of Pavement Engineering*, vol. 16, no. 8, pp. 710–720, 2014.
- [35] J. Zhang, Z. Li, H. Chu, and J. Lu, "A viscoelastic damage constitutive model for asphalt mixture under the cyclic loading," *Construction and Building Materials*, vol. 227, 2019.
- [36] H. Feng, M. Pettinari, and H. Stang, "Study of normal and shear material properties for viscoelastic model of asphalt mixture by discrete element method," *Construction and Building Materials*, vol. 98, pp. 366–375, 2015.